

Interpreting Radial Correlation Doppler Reflectometry using Gyrokinetic Simulations

J. Ruiz Ruiz¹, F. I. Parra¹, V. H. Hall-Chen¹, N. Christen¹, M. Barnes¹, J. Candy², J. Garcia³, C. Giroud⁴, W. Guttenfelder⁵, J. C. Hillesheim⁴, C. Holland⁶, N. T. Howard⁷, Y. Ren⁵, A. E. White⁷, and JET contributors⁸

¹Rudolf Peierls Centre for Theoretical Physics, University of Oxford, OX1 3NP, UK

²General Atomics, P.O. Box 85608, San Diego, CA, USA

³CEA, IRFM, F-13108 Saint-Paul-lez-Durance, France

⁴CCFE, Culham Science Centre, Abingdon, Oxon OX14 3DB, UK

⁵Princeton Plasma Physics Laboratory, Princeton, New Jersey 08543, USA

⁶Center for Energy Research, University of California, San Diego, La Jolla, California 92093-0417, USA

⁷MIT-Plasma Science and Fusion Center, Cambridge, Massachusetts 02139, USA

⁸See the author list of 'Overview of JET results for optimising ITER operation' by J. Mailloux *et al.* to be published in *Nuclear Fusion Special issue: Overview and Summary Papers from the 28th Fusion Energy Conference (Nice, France, 10-15 May 2021)*.

Radial correlation Doppler reflectometry (RCDR) [1] is a well established diagnostic technique to measure the radial correlation function in the turbulence, implemented via cross-correlation of neighboring Doppler backscattering signals. In Doppler backscattering, a microwave beam incident into the plasma at a finite incidence angle makes the backscattered signal sensitive to a specific turbulence wavenumber \mathbf{k}_\perp , which is related to the incident microwave beam wavenumber \mathbf{k}_i by the Bragg condition for backscattering at the cutoff $\mathbf{k}_\perp = -2\mathbf{k}_i$ [2, 3]. If the Doppler backscattering signal is sensitive to only one turbulence wavenumber \mathbf{k}_\perp , what does this mean for the measured radial correlation length? In this work, we study the dependence of the radial correlation length on the measured $k_\perp = |\mathbf{k}_\perp|$, and the potential diagnostic resolution effects on radial correlation length measurements via RCDR in the linear response regime [4, 5]. We use a synthetic model DBS applied to nonlinear gyrokinetic simulation corresponding to a highly unstable ETG regime in a moderate- β NSTX H-mode (analyzed in [6, 7, 9, 10]), and to an ITG-driven core turbulence regime in a JET L-mode (analyzed in [11]).

The model DBS implemented for gyrokinetic simulation assumes the scattered amplitude is a linear response with respect to the density fluctuations $A_s(\mathbf{r}_0, \mathbf{k}_0, t) = e^{-i\mathbf{k}_\perp \cdot \mathbf{r}_0} \sum_{\mathbf{k}_\perp} \delta\hat{n}(\mathbf{k}_\perp, \theta, t) W(\mathbf{k}_\perp - \mathbf{k}_{\perp 0})$, where W is a filter in \mathbf{k} -space applied to the density fluctuation field $\delta\hat{n}$ at the outboard midplane $\theta = 0$ (details in [12]). The perpendicular wave-vector is expanded along its normal k_n and binormal components k_b as $\mathbf{k}_\perp = k_n \mathbf{e}_n + k_b \mathbf{e}_b$, and $W(\mathbf{k}_\perp - \mathbf{k}_{\perp 0})$ is Gaussian in k_n and k_b , with characteristic radial resolution W_n and binormal resolution W_b . The model can be derived from a first principles, linear response, beam-tracing DBS model developed by Hall-Chen *et al.* [13].

We make the distinction between three different correlation functions. CCF^{real} is the *real* turbulence cross-correlation function, computed via radial correlation of the full density field δn from the gyrokinetic code for different radial separations Δx , and knows about the full turbulence spectrum (all \mathbf{k}_\perp). CCF^{k_b} is the scale-dependent correlation function corresponding to a specific turbulence wavenumber k_b , and informs about the characteristic radial correlation of a specific turbulent eddy with binormal wavenumber k_b . This quantity does not know about the full turbulence spectrum, but is intrinsic to k_b . Each binormal wavenumber k_b in the turbulence, ie. each binormal wavelength, has a specific radial structure associated to it, and it is given by CCF^{k_b} . The varying CCF^{k_b} for different k_b is an intrinsic characteristic of the turbulence, and it is *not* related to a diagnostic effect. CCF^{syn} is the synthetic cross-correlation function, computed via radial correlation of the scattered amplitude A_s . Notably this cross-correlation function is directly dependent on specific experimental parameters, which in this model are k_{b0} , W_n and W_b (here we use experimentally relevant $W_b \gg 2\pi/k_{b0}$). We will define the correlation length as the $1/e$ value of the corresponding radial correlation function.

Figure 1.a) shows the scale-dependent radial correlation length $l_r(k_b)$ computed from CCF^{k_b} for each individual k_b in the NSTX electron-scale gyrokinetic simulation (blue curve, where the $E \times B$ shearing rate $\gamma_E = 0$) along with the real correlation length of the turbulence (green dashed line, computed from CCF^{real}). The radial correlation length is largest for a finite

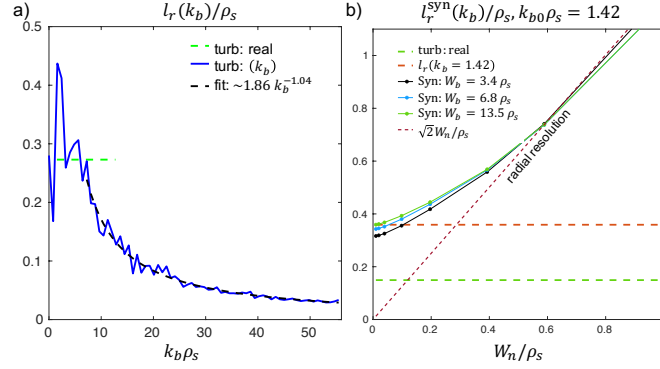


Figure 1: a) Scale-dependent $l_r(k_b)$ for the NSTX electron scale turbulence case. b) Synthetic correlation length as a function of W_n .

$k_b\rho_s \approx 1.5$, and it becomes a decreasing function of k_b for larger wavenumbers. A power law $\sim Ck_b^{-\alpha}$ is fitted to the l_r curve for larger wavenumbers ($k_b\rho_s \gtrsim 7$), giving an exponent $\alpha \approx 1.04$. This fit characterizes the scale-by-scale dependence of the radial correlation length corresponding to each binormal wavenumber k_b (or binormal wavelength). This shows that it is of crucial importance to take into account the scale by scale dependence of the radial correlation length as only one wavenumber k_b is selected by a Doppler reflectometer system. The relationship $l_r \sim Ck_b^{-\alpha}$ with $\alpha \approx 1$ implies that the radial characteristic length l_r and binormal wavenumber k_b preserve the same proportionality relation scale by scale (for $k_b\rho_s \gtrsim 7$). The constant of proportionality C can be interpreted as a rough measure of the eddy aspect ratio in the perpendicular (x, y) plane to \mathbf{B} . In this case we find $l_r/l_b \approx 1.54$, where $l_b \approx 1/k_b$. This estimate is only accurate when there is negligible tilt on the turbulence ($\gamma_E \approx 0$), and suggests that ETG-driven eddies measured by DBS would exhibit an aspect ratio $l_r/l_b \approx 3/2$ in the (x, y) plane (at the outboard midplane of this specific NSTX condition).

Next we seek to understand the effect of the filter's radial dimension W_n on the NSTX electron-scale turbulence simulation. Figure 1.b) shows the synthetic correlation lengths as a function of W_n (computed from CCF^{syn}) for different experimentally relevant values of the binormal spot size $W_b = 3.4, 6.8, 13.5 \rho_s$. The correlation length for small W_n converges to the correlation length for $k_b\rho_s = 1.42$ (red dashed line). However, for increasing W_n , the synthetic correlation length is shown to asymptote linearly to the purple dashed line, which is the radial resolution $\approx W_n$. This suggests that the diagnostic radial resolution W_n can itself strongly affect the value of the 'measured' correlation length in DBS experiments for large enough radial resolution W_n , when $W_n > l_r(k_{b0})$. The value of W_n in experiments remains an open question for Doppler backscattering. Previous work seems to suggest values on the order of the width of the Airy lobe W_{Ai} or the beam width, whichever is larger. It is well known that standard normal incidence reflectometry experiments are characterized by a radial spot size given by the width of the Airy lobe $W_{\text{Ai}} \approx 0.5L_\epsilon^{1/3}\lambda^{2/3}$ [14, 15], where L_ϵ is the permittivity scale length, equal to the density gradient scale length L_n in linear profile, slab geometry and O-mode polarization, and λ is the vacuum wavelength of the incident microwave beam. The issue of the width of the beam near the reflection point is discussed analytically in [16, 17], which seems to be supported by ray tracing, beam tracing and full-wave simulations carried out for realistic toroidal geometries of AUG [18, 19], additionally suggesting that the Airy width W_{Ai} should be considered as a minimum value of W_n in experiments. In the present conditions $W_{\text{Ai}} \approx 2\text{-}4 \rho_s$, which is notably larger than the largest correlation length in this strongly-driven ETG simulation condition ($l_r \approx 0.4 \rho_s$, figure 1.a)). This suggests that radial correlation length measurements carried out for electron-scale k_\perp DBS measurements are likely to be dominated by the radial resolution W_n , making impossible the measurement of the radial correlation length $l_r(k_b)$.

Similar features to the electron-scale turbulence can be observed in the JET ITG-driven ion-scale turbulence case, but this time for larger correlation lengths. The $1/e$ correlation length for each k_b is plotted in figure 2.a), in blue for $\gamma_E = 0$ and in red for $\gamma_E = \gamma_E^{\text{exp}}$. Both show a peak correlation length for $k_b\rho_s \approx 0.1\text{-}0.2$, and decreasing for larger k_b . The $\gamma_E = 0$ case exhibits larger l_r (γ_E can induce radial decorrelation), and yields slightly different values for the fit parameters. Inferring an eddy aspect ratio from the γ_E^{exp} case would yield an inaccurate estimate for l_r/l_b : the proportionality constant C in $l_r \sim Ck_b^{-\alpha}$ is only an accurate estimate the eddy aspect ratio when $\gamma_E \approx 0$ (due to the tilting of eddies induced by γ_E , details in [12]). The effect of finite diagnostic radial resolution W_n for ion-scale turbulence is similar to electron-scale turbulence, however, the condition $W_n < l_r(k_{b0})$ is now more easily satisfied. Figure 2.b) shows the variation of the $1/e$ synthetic correlation length with W_n . The correlation length converges to the correlation length of $k_{b0}\rho_s = 0.15$ for all values of W_b when $W_n \ll l_r(k_{b0})$,

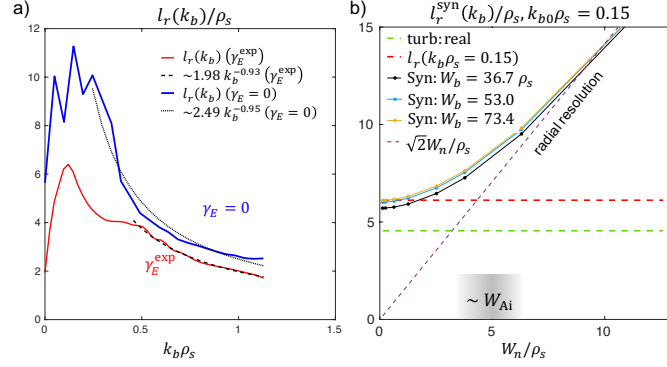


Figure 2: a) Scale-dependent $l_r(k_b)$ for the JET ion-scale turbulence case. b) Synthetic correlation length as a function of W_n .

and it asymptotes to the radial resolution W_n for $W_n \gg l_r(k_{b0})$. The condition $W_n \approx l_r(k_{b0})$ happens for a larger correlation length $l_r(k_{b0}\rho_s = 0.15) \approx 5 \rho_s$. Evaluating the reflectometry estimate for the radial spot size for the current conditions gives $W_n \approx W_{Ai} \approx 4-6 \rho_s$. This suggests that experimentally relevant W_n are likely to affect a measured RCDR correlation length, but in a less dramatic way than for electron-scale fluctuations. The effect is not be completely negligible, as demonstrated by figure 2.b).

The dependence of the radial correlation length on the binormal scale $l_r(k_b) \sim C k_b^{-\alpha}$ is encoded in the ensemble averaged turbulent wavenumber spectrum of the density fluctuations $\langle |\delta \hat{n}(k_n, k_b)|^2 \rangle_T$. This dependence can only be captured for non-separable density fluctuation spectra in k_n and k_b , ie. $\langle |\delta \hat{n}(k_n, k_b)|^2 \rangle_T \neq h_n(k_n)h_b(k_b)$ ([12]). Using a separable wavenumber spectrum, as in previous works [1, 4, 5] results in $l_r(k_b) = l_r^{\text{real}}$ for all k_b , which does not accurately represent magnetized plasma turbulence in the tokamak core. A proposed analytical expression for non-separable, density fluctuation wavenumber power spectra inspired from the power-law spectra characteristic of gyrokinetic simulations, and which contains the scale-by-scale dependence of the radial correlation length, is as follows

$$\langle |\delta \hat{n}/n(k_n, k_b)|^2 \rangle_T \sim \frac{A}{1 + \left(\frac{|k_n|}{w_{k_n}}\right)^\gamma + \left(\frac{|k_b - k_{b*}|}{w_{k_b}}\right)^\beta} \quad \Rightarrow \quad l_r(k_b) \sim \frac{\text{const.}}{w_{k_n}} \frac{1}{\left[1 + \left(\frac{|k_b - k_{b*}|}{w_{k_b}}\right)^\beta\right]^{1/\gamma}}. \quad (1)$$

In this expression, the spectral exponents γ and β in k_b are allowed to differ, w_{k_n} and w_{k_b} represent the spectral widths of the turbulence wavenumber spectrum, and the spectrum in k_b is allowed to peak at a finite $k_b = k_{b*}$, consistent with the linear drive for typical micro-instabilities in the tokamak core peaking at finite values of k_b , and representing the injection driving scale of the turbulence (eg. $k_{b*}\rho_s \approx 0.1-0.6$ for ITG, $k_{b*}\rho_s \approx 2-30$ for ETG, etc.). The analytic expression of the spectrum allows an analytic expression of $l_r(k_b)$, which has the functional dependence exhibited in equation 1.

In figure 3.a) are shown the scale-dependent correlation functions CCF^{k_b} of the gyrokinetic (thick lines) and analytic spectra fit (colored dots), corresponding to two different wavenumbers $k_b\rho_s = 3.22, 13.67$ in the NSTX electron-scale turbulence condition. The scale-dependent correlation functions are satisfactorily reproduced by the analytic expression for the spectrum. The scale-dependent correlation length $l_r(k_b)$ computed for all k_b is also shown to be well reproduced by the analytic spectrum in equation (1), as is shown in figure 3.b). This discussion motivates a preferential use of realistic spectra, gyrokinetic or analytic expressions as in equation (1), above the use of separable spectra (Gaussian, Lorentzian, top-hat, etc.) in future modelling works of RCDR. Similar analysis for the JET ion-scale turbulence condition also shows satisfactory agreement of the analytic spectrum with the gyrokinetic spectrum.

The proposed relationship $l_r(k_b) \sim k_b^{-\alpha}$ appears to be a universal, robust characteristic of the turbulence, as provided by nonlinear gyrokinetic simulation of ETG and ITG-driven turbulence. This may explain, or contribute to the explanation of, the observed decrease of the measured radial correlation length with k_b in experiments [20] (denoted k_\perp in the literature). The fact that analytical work [5] and full-wave simulations [21] show that separable spectra (Gaussian, top-hat, Lorentzian, etc.) yield a measured l_r dependent on k_b suggests that a combination of two effects, the scale-by-scale variation of l_r with k_\perp and a diagnostic effect (forward scattering [5]) may explain the experimental observations [20]. For this reason, an analytic,

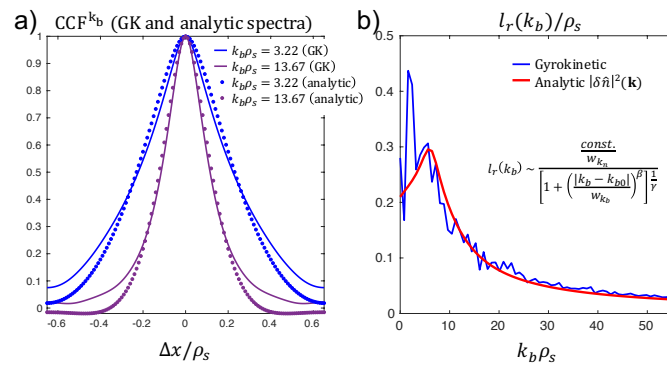


Figure 3: **a)** Scale-dependent correlation function CCF^{k_b} computed from gyrokinetic simulation (thick lines), compared to CCF^{k_b} using analytic fit to the wavenumber spectrum (colored dots). **b)** Scale-dependent correlation length for all wavenumbers k_b in the simulation.

realistic power-law spectrum (equation (1)) is proposed, which could be used in future works to model the DBS response using full-wave or analytical calculations.

The author would like to thank the whole NSTX team for providing the profile data used for the analysis of the plasma discharge presented here. Discussions with T. Estrada and D. Carralero have also been insightful for the preparation of this manuscript. This work has been supported by U.S. D.O.E. contract DE-AC02-09CH11466, and in part by the Engineering and Physical Sciences Research Council (EPSRC) [EP/R034737/1]. Computer simulations were carried out at the National Energy Research Scientific Computing Center, supported by the Office of Science of the U.S. D.O.E. under Contract No. DE-AC02-05CH11231, at the MIT-PSFC partition of the Engaging cluster at the MGHPC facility (www.mghpc.org), which was funded by D.O.E. grant number DE-FG02-91-ER54109, and the supercomputer ARCHER in the UK, which was funded by EPSRC [EP/R034737/1]. This work has been carried out within the framework of the EUROfusion Consortium and has received funding from the Euratom research and training programme 2014-2018 and 2019-2020 under grant agreement No 633053. The views and opinions expressed herein do not necessarily reflect those of the European Commission.

References

- [1] J. Schirmer *et al.*, Plasma Phys. Control. Fusion **49** 1019 (2007).
- [2] E. Holzhauser *et al.*, Plasma Phys. Control. Fusion **40** 1869 (1998).
- [3] M. Hirsch *et al.*, Review of Scientific Instruments **72**, 324 (2001).
- [4] E. Z. Gusakov and A. V. Surkov, Plasma Phys. Control. Fusion **46**, 1143 (2004).
- [5] E. Gusakov, M. Irzak and A. Popov, Plasma Phys. Control. Fusion **56**, 025009 (2014).
- [6] J. Ruiz Ruiz *et al.*, Phys. Plasmas **22**, 122501 (2015).
- [7] J. Ruiz Ruiz *et al.*, Plasma Phys. Control. Fusion **61**, 115015 (2019).
- [8] J. Ruiz Ruiz *et al.*, Plasma Phys. Control. Fusion **62**, 075001 (2020).
- [9] J. Ruiz Ruiz *et al.*, Phys. Plasmas **27**, 122505 (2020).
- [10] Y. Ren *et al.*, Nucl. Fusion **60**, 026005 (2020).
- [11] N. Christen *et al.*, J. Plasma Phys. **87**(2), (2021).
- [12] J. Ruiz Ruiz *et al.*, in preparation.
- [13] V. Hall-Chen *et al.*, in preparation.
- [14] I. H. Hutchinson, Plasma Phys. Control. Fusion **34** 1225 (1992).
- [15] R. Nazikian *et al.*, Physics of Plasmas **8**, 1840 (2001).
- [16] O. Maj *et al.*, Phys. Plasmas **16**, 062105 (2009).
- [17] O. Maj *et al.*, Plasma Phys. Control. Fusion **52**, 085006 (2010).
- [18] G. D. Conway *et al.*, Proc. 12th Intl. Reflectometry Workshop - IRW12, Julich (2015).
- [19] G. D. Conway *et al.*, Proc. 14th Intl. Reflectometry Workshop - IRW14, Lausanne, (2019).
- [20] F. Fernández-Marina, T. Estrada and E. Blanco, Nucl. Fusion **54** 072001 (2014).
- [21] E. Blanco and T. Estrada, Plasma Phys. Control. Fusion **55**, 125006 (2013).